

OUTDOOR PROPAGATION

REVIEW OF PHYSICAL MECHANISM AND COMPUTATIONAL MODELS

Gilles A. Daigle

Institute for Microstructural Sciences, National Research Council
Ottawa, Ontario K1A 0R6

INTRODUCTION

Propagation of noise in the atmosphere is governed by a number of interacting physical mechanisms including geometrical spreading, molecular absorption, reflection from a porous ground, curved ray paths due to refraction, diffraction by ground topography and scattering by turbulence. Accurate predictions of noise levels from a distant source must somehow account for all of these phenomena simultaneously. Although this goal is still beyond current capabilities, developments in computational tools for predicting sound propagation through the atmosphere have increased dramatically during recent years. The computational techniques now include analytical solutions for selected atmospheric profiles, ray tracing techniques which include interaction with the ground and meteorological conditions, and more sophisticated numerical solutions to the full wave equation; the fast field program (FFP) and the parabolic equation (PE). With modern computers, it is now becoming practical to incorporate some of these new computational tools into predictions schemes with advantages such as calculated noise contours based on observed meteorological patterns.

All noise prediction models include the attenuation due to geometrical spreading and, if required, molecular absorption. Where the empirical based models differ from computational models is in the incorporation of the other attenuation mechanisms. The empirical models tend to rely on general tendencies found in experimental databases. They often work well as long the specific situation of interest falls within the bounds of the databases. Computational models on the other hand rely on our mathematical ability to describe real-life situations. Recently the status of the computational methods was reviewed [1] and Benchmark cases to check performance and accuracy have been defined [2]. The purpose of this paper is to review the new computational models. The paper summarizes their limitations, their advantages, and shows a benchmark comparison of predictions. A complete and detailed description of each model, including comparison with experimental data, can be found in the cited references.

THEORETICAL BACKGROUND

The computational models assume simple harmonic time dependence $\exp(-i\omega t)$ and begin with the Helmholtz equation

$$[\nabla^2 + k^2]p(r, z) = -4\pi\delta(r, z - z_s) \quad (1)$$

where the wavenumber $k(z) = \omega/c(z)$, r is the horizontal range and z is the height above the ground. Reflection from a porous ground is described by the boundary condition

$$[\partial p / \partial z + ik\beta p]_{z=0} = 0 \quad (2)$$

at the ground surface where β is the normalized complex surface

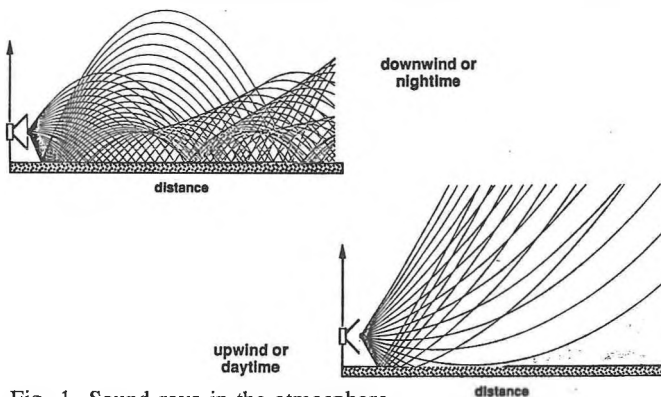


Fig. 1 Sound rays in the atmosphere

admittance. In general, the speed of sound varies with height resulting in curved ray paths due to refraction as shown in Fig 1. During nighttime or downwind propagation, ray paths are curved downward leading to multiple rays and favourable propagation conditions. During daytime or upwind propagation, ray paths are curved upward leading to an acoustic shadow with increased attenuation. The atmosphere is also turbulent, requiring the wavenumber to be separated into deterministic and stochastic parts, $k(z) = k_0(n_d + \mu)$, where n_d is the refractive index and μ a small perturbation. Turbulence scatters sound energy into shadows produced by barriers or refraction, limiting the amount of attenuation. Finally, terrain, such as berms or barriers, can be incorporated through boundary conditions or range dependence.

DESCRIPTION OF THE MODELS

The computational models describe below differ in their mathematical origin and in the way some of the physical mechanisms are incorporated. For example, some of the models are limited to a specific functional form for the sound speed profile. Some of the models do not include turbulence. All the models incorporate the boundary condition Eq. (2) in some way. The different approaches are presented following Ref. [2].

Analytical wave solutions

The Helmholtz equation (1) can be solved with a zero-order Hankel transform

$$p(r, z) = - \int H_0^1(Kr) P(K, z) K dK \quad (3)$$

Residue series solutions to Eq. (2) can be found when the sound speed is assumed to vary linearly with height. The residue solutions do not incorporate turbulence (i.e., $\mu = 0$). The downward refraction solution is called Normal Modes [3] while the upward refraction solution is described in terms of Creeping Waves [4]. The solutions usually converge rapidly. An example of how noise levels of a few hundred Hz are predicted to decrease with distance (Transmission Loss, TL) according to the Normal Mode solution is shown for a benchmark case [2] in Fig. 2(c).

In the case where the sound speed is constant with height above the ground, ray paths are straight and the solution Eq. (3) reduces to the more familiar sum of direct and ground reflected waves [5]

$$p(r) = A_d \exp(ikr_d)/r_d + Q(\beta, \phi) A_r \exp(ikr_r)/r_r \quad (4)$$

where r_d and r_r are the path length of the direct and reflected path, respectively, Q is the reflection coefficient and ϕ is the angle of incidence. In reality though, ray paths are rarely straight and Eq. (4) is usually not valid at distances beyond a few hundred meters.

Ray tracing solutions

The effects of curved ray paths can be described from general principles. The curved ray modifies the angle of incidence and Eq. (4) can be used along with basic ray theory to construct heuristic physical solutions. Ray tracing solutions are computationally efficient. We note, however, that ray theory will not work beyond the shadow boundary in the case of upward refraction. The TL predicted from such a heuristic solution [6] for the downward refraction benchmark case is shown in Fig. 2(a). The heuristic model assumes the sound speed to vary linearly with height and can incorporate turbulence. The restriction of a linear sound speed profile can be removed if the ray solution is restricted to only one ground reflected ray. However this limits the validity to shorter distances [2].

The Gaussian beam approach [7] is another variation of ray tracing solutions. The basic concept of the theory is to launch a fan of ray-centered beams from the source and to trace the propagation of these beams through the medium. The wave equation is solved

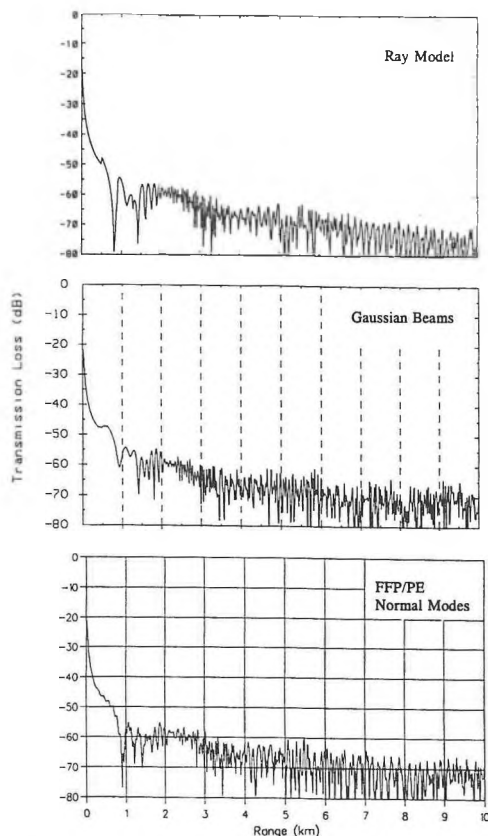


Fig. 2 Benchmark cases for downward refraction

in the immediate vicinity of each ray and the acoustic pressure at the receiver is obtained by summing the contribution of each of the individual beams. The Gaussian beam model can assume an arbitrary sound speed profile but the current implementation does not incorporate turbulence. The TL predicted by the Gaussian beam model for the benchmark case is shown in Fig. 2(b). We note that this model is effective in predicting the loss of performance of barriers where rays curve over the top of the barrier edge due to refraction [7].

FFP models

Fast Field Programs (FFP) performs a direct numerical integration on Eq. (4). They allow the prediction of noise levels in a horizontally stratified atmosphere where the sound speed is an arbitrary function of height. Current implementations are restricted to a flat ground with range-independent properties that assume a non-turbulent atmosphere. Four adaptations of the FFP are called CERL-FFP [8], SAFARI [9], CFFP [10], and FFLAGS [11]. The CERL-FFP and CFFP treat the ground surface as a locally reacting impedance boundary while FFLAGS permits ground layering and elasticity in addition to porosity. The SAFARI FFP only allows layering and elasticity.

The three FFPs that assume porous ground predict the curve in Fig. 3(c) for the benchmark case. SAFARI predicts less Transmission Loss because of the assumption of a non-porous ground. The FFPs generally provide accurate prediction but are computationally time consuming. Further, the assumption of a non-turbulent atmosphere seriously restricts the use of the FFPs in the case of upward refraction.

PE models

The Parabolic Equation (PE) employs an assumption that wave motion for a particular problem is always directed away from the source or that there is very little backscattering. Writing $U = pr^{1/2}$, the Helmholtz equation in cylindrical coordinates is factored into propagation of incoming and outgoing waves. Considering

only the outgoing wave leads to the *one-way wave equation*

$$\partial U / \partial r = i \sqrt{q} U \quad (5)$$

where $q = \partial^2 / \partial z^2 + k^2$. Most implementations of the PE can be traced back to Eq. (5). The approach for advancing the field in range is the point of departure for the PE methods. Two popular software implementations are called FINITE-PE [12] and FAST-PE [13]. The FINITE-PE method numerically integrates Eq. (5) using a Crank-Nicolson approach. The boundary condition Eq. (2) must be satisfied at each step requiring several integration steps per wavelength to model the large variations of the field close to the boundary and results in computation times comparable to the FFPs. The FAST-PE uses a Green's function approach and a split-step operation that factors \sqrt{q} into an operator for a homogeneous medium and another operator for propagation through the inhomogeneous perturbation. In addition, there are explicit terms for the field reflected from the ground allowing range steps of several wavelengths which results in dramatically decreased computation time.

The PEs allow the prediction of noise levels in a turbulent atmosphere [15] where the sound speed is an arbitrary function of height. Current developments are aimed at incorporating terrain [16,17]. In the case of the downward refraction benchmark case the PEs yield the curve in Fig. 2(c). In the case of upward refraction, models that neglect atmospheric turbulence predict large attenuations at longer ranges that are not supported by experimental data [18]. In the case of an upward refracting turbulent atmosphere the curves in Fig. 3 are typical levels [14] predicted for three values of the parameter μ . In essence, the relative sound pressure levels (SPL) in Fig. 3 represent the attenuation in excess of the transmission loss shown in Fig. 2 due to upward refraction.

SUMMARY

When experimental data is sufficiently documented to allow comparison with the computational models, good agreement is obtained for a wide variety of situations and conditions [8,18,19]. The speed of modern computers, the increase accuracy and reliability are making the use of computational models cost effective alternatives for noise prediction schemes. We are beginning to see effort directed at predicting the hourly, daily, or seasonal variations in noise levels due to changes in environmental conditions by incorporating local weather into predictions schemes using computational models.

REFERENCES

- [1] G.A. Daigle et al., J. Acoust. Soc. Am. **92**, 2404 (1992).
- [2] K. Attenborough et al., submitted to J. Acoust. Soc. Am.
- [3] R. Raspet et al., J. Acoust. Soc. Am. **91**, 1341 (1992).
- [4] A. Berry and G.A. Daigle, J. Acoust. Soc. Am., **83**, 2047 (1988).
- [5] K. Attenborough et al., J. Acoust. Soc. Am., **68**, 1493 (1980).
- [6] A. L'Espérance et al., Appl. Acoust. **37**, 111 (1992).
- [7] Y. Gabillet et al., **93**, 3105 (1993).
- [8] S. W. Lee et al., J. Acoust. Soc. Am. **79**, 628 (1986).
- [9] A. Güdesen, J. Acoust. Soc. Am. **87**, 1968 (1990).
- [10] Y. L. Li et al., J. Acoust. Soc. Am. **89**, 2068 (1991).
- [11] S. Tooms et al., J. Acoust. Soc. Am. **93**, 173 (1993).
- [12] K.E. Gilbert and M.J. White, J. Acoust. Soc. Am. **85**, 630 (1989).
- [13] K.E. Gilbert and X. Di, J. Acoust. Soc. Am. **93**, 714 (1992).
- [14] X. Di and G.A. Daigle, Proc. INTER-NOISE 94.
- [15] K.E. Gilbert et al., J. Acoust. Soc. Am. **87**, 2428 (1990).
- [16] Craddock and White, J. Acoust. Soc. Am. **91**, 3184 (1992).
- [17] E.M. Salomons, J. Acoust. Soc. Am. **95**, 3109 (1994).
- [18] White and Gilbert, Appl. Acoust. **27**, 227 (1989).
- [19] A. L'Espérance et al., Appl. Acoust. **40**, 325 (1993).

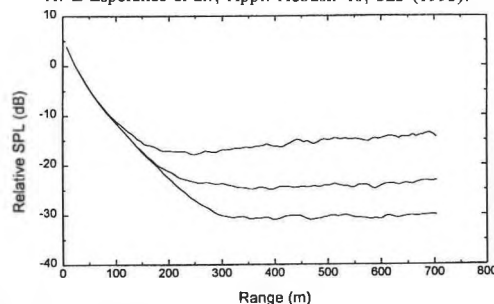


Fig. 3 Typical predictions in the case of upward refraction